Theoretical Study of the Cyclopropenyl Radical[1]

Daniel M. Chipman* and Kristine E. Miller

Contribution from the Radiation Laboratory, University of Notre Dame, Notre Dame, Indiana 46556. *Received February 24, 1984*

Abstract: Comprehensive ab initio MCSCF and CI calculations are performed to determine properties of the cyclopropenyl radical, which has not yet been directly observed experimentally. Jahn-Teller distortion is responsible for a dramatic change from the high-symmetry D_{3h} π radical parent structure to a low-symmetry nonplanar C_s σ radical equilibrium structure. The equilibrium structure is found to be an ethylenic form that can exist in three equivalent conformations. These can interconvert (via a pseudorotation of the carbon-carbon double bond around the ring) by passing through a nonplanar allylic transition state. Planar geometries turn out to be of such high energy as to play no significant role in the dynamics of this system. Large-scale CI calculations, with corrections for differences in zero-point vibrational energies, indicate the pseudorotation barrier height to be about 3-4 kcal/mol. Qualitative results are obtained for the energy and geometry changes that occur along the interconversion path. A number of one-electron properties are also reported for the equilibrium form. Notable among these are the spin-density predictions, which should be of use in experimental identification of the cyclopropenyl radical by ESR spectroscopy. A qualitative survey of the energies and geometries of other C_3H_3 isomers is also presented.

I. Introduction

Recently reported experimental observations of the trimethyl[2,3] and dimethyl[3] derivatives of the cyclopropenyl radical have stimulated interest in the unsubstituted radical itself. The latter has not yet been observed directly, although its presence has been inferred in voltammetric measurements[4] based on the parent cation. In the absence of any direct experimental information on the properties of the neutral radical, it is necessary to resort to theoretical studies. The purpose of this paper is to utilize quantum chemical calculations of sufficient reliability to provide semiquantitative predictions of the energies, geometries, spin densities, and other properties for the relevant forms of cyclopropenyl radical.

The Jahn-Teller effect is responsible for dramatic changes in the structure and properties of this system. Formally adding an electron to the highly symmetric D_{3h} structure of the parent cation would give the neutral π radical in an E state, with the unpaired electron in either of two degenerate π orbitals. The subsequent Jahn-Teller distortion apparently completely changes the nature of the system to that of a low-symmetry C_s σ radical (see Figure 1). Also of considerable interest is the decrease in the number of observed unique hydrogen hyperfine coupling constants upon warming the trimethyl derivative,[2,3] indicating a low energy barrier to internal conversion among equivalent equilibrium structures.

Several early theoretical discussions[5] of the Jahn-Teller distortion of the cyclopropenyl radical considered only planar structures, wherein the two degenerate $^2E_x''$ and $^2E_y''$ states of D_{3h} symmetry would be expected to distort to π radicals in $^2A_1$ (ethylenic) and $^2B_2$ (allylic) states of C_{2v} symmetry (see Figure 1). Recently, Davison and Borden[6] have presented a highly instructive formal analysis of these planar states. These workers also carried out minimal basis CI calculations showing the ethylenic form to be the most stable and suggesting that the slightly higher energy (by 1 kcal/mol) allylic form is a transition state for interconversion among the three possible equivalent ethylenic structures. This interconversion process corresponds to pseudorotation of the ethylenic double bond around the three ring bond positions.

A recent computational study by Hoffmann et al.[7] has addressed the difficulties inherent in calculating wave functions of D_{3h} symmetry for the parent system. Ordinarily, it is feasible only to constrain the wave functions to C_{2v} symmetry, with the result that the two theoretically degenerate states at a D_{3h} geometry will be subject to symmetry breaking and a spurious energy splitting will be calculated.

Other calculations have considered nonplanar geometries[8,9,10] and found the most stable form to be a σ radical of C_s symmetry, in accord with the interpretation given to the experimental results on the trimethyl derivative.[2,3] The ab initio ROHF calculations of Baird[9] and the UHF, ROHF, and single-excitation CI calculations of Poppinger et al.[10] both indicate the $^2A'$ (ethylenic) form to be more stable than the $^2A''$ (allylic) form (see Figure 1) and that each of these is considerably more stable than its planar counterpart. Poppinger et al.[10] speculate that the $^2A''$ allylic form may be the transition state for pseudorotation.

The present study generally confirms the qualitative conclusions alluded to above while providing a much more complete and quantitative picture of the potential surface and properties of the cyclopropenyl radical. The major new theoretical feature here is the use of a more reliable reference wave function than has heretofore been utilized. In the Appendix, it is shown that the commonly used UHF and ROHF models are each subject to symmetry instabilities for this system and that, even when symmetry constrained, they give qualitatively incorrect results for the energy barrier to pseudorotation. Both of these difficulties are resolved by the MCSCF model used here. Particular attention is also paid to basis set requirements for reliable calculations on this system. Full computational details are provided in section II.

In section III the Jahn-Teller distortion is studied by calculating MCSCF energies and optimized geometries for the relevant D_{3h}, C_{2v}, and C_s forms of cyclopropenyl radical. It is found there that the C_s ethylenic form is the equilibrium geometry and that planar D_{3h} and C_{2v} forms are too high in energy to play any significant role in the actual dynamics of this system. The optimum ethylenic and allylic C_s geometries are calculated with large basis sets including polarization functions.

Full vibrational analyses are performed at the stationary ethylenic and allylic points of C_s symmetry in section IV. These show unequivocally that the ethylenic form is a local minimum

(1) This research was supported by the Office of Basic Energy Science of the U. S. Department of Energy. This is Document No. NDRL-2556 from the Notre Dame Radiation Laboratory.

(2) Closs, G. L.; Evanochko, W. T.; Norris, J. R. *J. Am. Chem. Soc.* **1982**, *104*, 350.

(3) Sutcliffe, R.; Lindsay, D. A.; Griller, D.; Walton, J. C.; Ingold, K. U. *J. Am. Chem. Soc.* **1982**, *104*, 4674.

(4) Wasielewski, M. R.; Breslow, R. *J. Am. Chem. Soc.* **1976**, *98*, 4222.

(5) (a) Snyder, L. C. *J. Phys. Chem.* **1962**, *66*, 2299. (b) Liehr, A. D. *Annu. Rev. Phys. Chem.* **1962**, *13*, 41. (c) Ha, T.-K.; Graf, F.; Gunthard, H. H. *J. Mol. Struct.* **1973**, *15*, 335. (d) Cirelli, G.; Graf, G.; Gunthard, H. H. *Chem. Phys. Lett.* **1974**, *28*, 494. (e) Pancir, J.; Zahradnik, R. *Tetrahedron* **1976**, *32*, 2257.

(6) (a) Davidson, E. R.; Borden, W. T. *J. Chem. Phys.* **1977**, *67*, 2191. (b) Davidson, E. R.; Borden, W. T. *J. Phys. Chem.* **1983**, *87*, 4783.

(7) Hoffmann, M. R.; Laidig, W. D.; Kim, K. S.; Fox, D. J.; Schaefer, H. F. *J. Chem. Phys.* **1984**, *80*, 338.

(8) Shanshal, M. *Z. Naturforsch., A* **1971**, *26*, 1336.

(9) Baird, N. C. *J. Org. Chem.* **1975**, *40*, 624.

(10) Poppinger, D.; Radom, L.; Vincent, M. A. *Chem. Phys.* **1977**, *23*, 437.

0002-7863/84/1506-6236$01.50/0

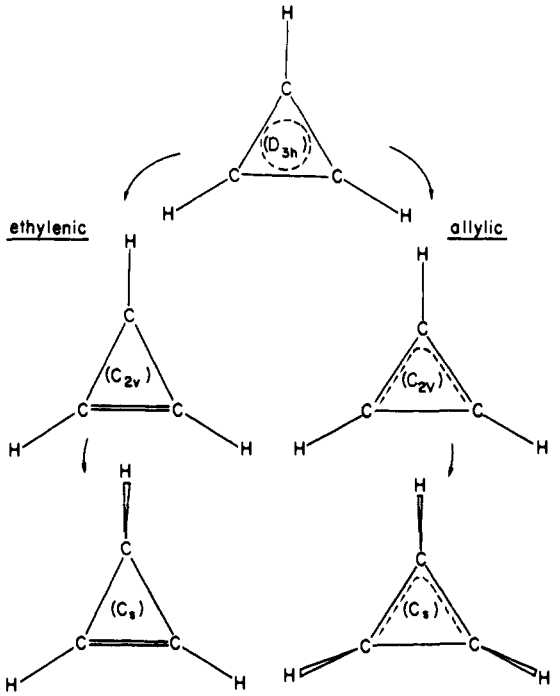

Figure 1. Jahn–Teller distortion of the cyclopropenyl radical.

and the allylic form is the transition state for pseudorotation. In section V the changes in energy and geometry are calculated for various points along the pseudorotation path. It is found that most of the hydrogen atom motions occur in a small region near the allylic transition state.

In section VI large-scale CI calculations are performed at the stationary MCSCF ethylenic and allylic C_s geometries to provide a more quantitative estimate of the energy barrier to pseudorotation. These lead to a result of 4.9 kcal/mol. Combining this electronic contribution with a lowering of 1.4 kcal/mol due to the difference in zero-point energies, we arrive at our final best prediction of about 3–4 kcal/mol for the barrier to be observed experimentally.

A number of one-electron properties calculated for the equilibrium C_s ethylenic form of the cyclopropenyl radical are presented in section VII. Of particular interest are the predicted ESR hyperfine coupling constants (hfc), which should be useful in the verification of any possible experimental identification of this species.

Included in the Appendix is a crude qualitative survey of a number of possible C_3H_3 isomers. This helps to put the cyclopropenyl radical in better perspective as part of the full potential energy surface for this system. The qualitative failures of UHF- and ROHF-based calculations for this system are examined there also.

II. Computational Details

It is possible that the difficulties with the UHF and ROHF methods (see the Appendix for a full discussion) may become less severe or even disappear with the use of larger basis sets and/or CI or perturbation theory corrections. However, we have found a more satisfying resolution to these difficulties in the use of a MCSCF reference model. Cation RHF calculations on both the ethylenic and allylic C_s forms indicate the highest doubly occupied MO and the two lowest (negative energy) unoccupied MO's (which latter accommodate the unpaired electron in the two forms of the neutral radical) are all dominated by large coefficients of carbon "π" AO's. These three MO's are the descendants of the π MO's found at planar geometries, although of course a strict σ–π separation does not apply at the nonplanar geometries. These can then be considered the active or frontier orbitals of this system, and in the main body of this work we utilize wave functions obtained by MCSCF optimization of the orbitals in all configurations obtained by distributing three electrons among these three MO's. This corresponds to optimization in the complete active configuration space generated within the conceptual minimal basis of those MO's dominated by the three carbon "π" AO's. In general this leads to an eight-configuration expansion of the wave function. At symmetric C_s, C_{2v}, and D_{3h} geometries the eight are divided into four configurations of one symmetry and four of another.

This small MCSCF model is found to give quite good results even with minimal basis sets, as evidenced by the small corrections found on proceeding to large basis sets and to inclusion of large-scale CI, and it is used throughout the main body of this paper. Basis sets used include the minimal STO-3G basis[11] and the split-valence 3-21G basis[12] developed by Pople's group, the split valence [32|2] and double-ζ [42|2] bases contracted by Dunning[13] from Huzinaga's[14] primitive sets, and [321/2] and [421/2] bases formed by adding d-polarization functions of exponent 0.75 to the carbon atoms. Most MCSCF calculations were performed with the GAMESS[15] package, which utilizes analytic gradients for geometry optimization and finite first differences of analytic gradients for force constants. Some single-point CI calculations were performed with the Ohio State–Argonne[16] programs kindly supplied by Dr. R. Shepard. Property-expectation values were obtained from a program interfaced by us to the latter system.

III. Jahn–Teller Distortion

The geometry of the parent structure was optimized within D_{3h} symmetry, but due to program limitations the wave functions were constrained only to the lower symmetry C_{2v} subgroup. Thus, the desired $^2E_x''$ wave function of D_{3h} symmetry was actually computed as a $^2B_1$ wave function of C_{2v} symmetry (which correlates with the allylic form), and the desired $^2E_y''$ wave function of D_{3h} symmetry was actually computed as a $^2A_2$ wave function of C_{2v} symmetry (which correlates with the ethylenic form). As a consequence, the theoretically degenerate $^2E''$ states were actually computed to have slightly different energies due to differential polarization effects on the core electrons. The computed energies of both states were then necessarily lower than properly constrained D_{3h} calculations (with the same configurations) would give. Detailed discussions of these points are available in the literature.[6,7]

Fortunately, as seen in Table I, these artificial differential polarization effects at D_{3h} geometries turned out to be minor. The two computed states were found to have essentially identical optimum D_{3h} geometries and to have energies differing by only 0.2 kcal/mol with the STO-3G basis and 0.6 kcal/mol with the 3-21G basis. In both cases the form with the allylic wave function was the lowest in energy. The 3-21G (split-valence) basis predicts a somewhat shorter CH bond and somewhat less instability relative to equilibrium cyclopropenyl than does the STO-3G (minimal) basis. In view of the fact that properly constrained wave functions for the D_{3h} calculations would lead to even higher energies, it can be concluded that D_{3h} geometries are $\gtrsim$20 kcal/mol less stable than the equilibrium form and so should play a negligible role in the actual dynamics of the cyclopropenyl radical.

Allowing the geometry to relax while maintaining C_{2v} symmetry leads (with no energy barriers) to distinctly different planar ethylenic ($^2A_2$) and allylic ($^2B_1$) geometries, as seen in Table I. Each form is lowered by $\sim$7–8 kcal/mol relative to the D_{3h} forms. The STO-3G basis predicts ethylenic to be more stable than allylic by 0.8 kcal/mol, while the larger 3-21G basis predicts allylic to be more stable by 0.1 kcal/mol. The ordering is thus too close to call from calculations at this level, and we can only reiterate the finding of Davidson and Borden[6] that the potential surface of planar cyclopropenyl is very flat. In any case, we do not consider it important to pursue this question further since the planar forms are >10 kcal/mol less stable than the equilibrium form and so should be of little importance for the actual dynamics of this system.

One might expect pyramidalization at those carbon atoms having significant unpaired electron density, and it is seen in Table I that this is indeed the case. Allowing the planar C_{2v} forms to relax to nonplanar C_s geometries causes (with no energy barriers)

(11) Hehre, W. J.; Stewart, R. F.; Pople, J. A. *J. Chem. Phys.* **1969**, *51*, 2657.
(12) Binkley, J. S.; Pople, J. A.; Hehre, W. J. *J. Am. Chem. Soc.* **1980**, *102*, 939.
(13) Dunning, T. H. *J. Chem. Phys.* **1970**, *53*, 2823.
(14) Huzinaga, S. *J. Chem. Phys.* **1965**, *42*, 1293.
(15) Dupuis, M.; Spangler, D.; Wendoloski, J. J. *NRCC Software Catalog* **1980**, *1*, Prog. No. QG01, GAMESS.
(16) Lischka, H.; Shepard, R.; Brown, F. B.; Shavitt, I. *Int. J. Quantum Chem., Quantum Chem. Symp.* **1981**, *15*, 91.

Table I. Energies and Optimized Geometries of the Cyclopropenyl Radical, As Obtained from ab Initio MCSCF Calculations[a]

basis set	total energy	relative energy	$R_{12} = R_{13}$	R_{23}	r_4	$r_5 = r_6$	θ_4	$\theta_5 = \theta_6$	$\phi_5 = \phi_6$
			D_{3h}						
STO-3G	−113.7560, −113.7563[b]	24.2, 24.1[b]	1.415	1.415	1.072	1.072	(0)	(0)	(0)
3-21G	−114.5240, −114.5248[b]	18.4, 17.9[b]	1.415	1.415	1.056	1.056	(0)	(0)	(0)
			C_{2v} Ethylenic						
STO-3G	−113.7698	15.6	1.461	1.329	1.066	1.076	(0)	(0)	−0.4
3-21G	−114.5363	10.7	1.471	1.324	1.053	1.059	(0)	(0)	−0.2
			C_{2v} Allylic						
STO-3G	−113.7685	16.4	1.373	1.501	1.080	1.069	(0)	(0)	0.3
3-21G	−114.5365	10.6	1.369	1.527	1.062	1.055	(0)	(0)	−0.1
			C_s Ethylenic						
STO-3G	−113.7946	(0)	1.473	1.318	1.089	1.075	47.8	0.7	0.5
3-21G	−114.5533	(0)	1.484	1.316	1.073	1.058	46.3	−0.1	0.4
[32|2]	−115.1679	(0)	1.491	1.332	1.075	1.062	43.8	−0.3	0.7
[321|2]	−115.2275	(0)	1.465	1.315	1.082	1.070	45.5	0.4	0.9
			C_s Allylic						
STO-3G	−113.7831	7.2	1.385	1.507	1.079	1.081	6.0	34.0	4.5
3-21G	−114.5434	6.2	1.377	1.532	1.061	1.065	5.0	30.9	3.8
[32|2]	−115.1599	5.0	1.392	1.534	1.064	1.067	5.3	29.6	3.4
[321|2]	−115.2198	4.9	1.374	1.506	1.073	1.074	6.3	32.9	4.8

[a] Refer to Figure 2 for notation. Total energies are in atomic units, relative energies are given in kcal/mol relative to the C_s ethylenic form with the same basis, bond lengths are in angstroms, and all angles are in degrees. [b] The D_{3h} energies are given first for the ethylenic and then for the allylic wave function. See text for discussion.

the hydrogen atom bonded to the apex carbon of the ethylenic ($^2A'$) form to bend about 45 deg away from the carbon ring plane and the two equivalent hydrogens of the allylic ($^2A''$) form to bend about 30°. There is little or no bending at positions of low unpaired electron density, the two equivalent hydrogens of the ethylenic form remaining essentially in the plane and the unique hydrogen of the allylic form bending only about 5° to the same side of the plane as the other two hydrogens. This pyramidalization lends over 10 kcal/mol more stability to the ethylenic form and about 5 kcal/mol or more stability to the allylic form.

At the final nonplanar C_s geometries, there is a very clear preference for the ethylenic over the allylic form by about 5 kcal/mol. The net result of Jahn–Teller distortion is then to cause large geometry changes in the parent π radical, ultimately leading to a much more stable σ-radical equilibrium structure.

The C–C bond length of 1.415 Å at the D_{3h} geometry is typical of a conjugated bond. At the ethylenic geometries the nominal C–C single bond lengths range around 1.46–1.49 Å, depending on the calculation, which is a little shorter than a normal single bond, while the C–C double bond ranges around 1.31–1.33 Å and is close to a normal double bond. At the allylic geometries the two C–C bond lengths ranging around 1.36–1.39 Å are normal for conjugated bonds and the C–C single bond lengths ranging around 1.50–1.53 Å are normal for a single bond.

The C–H bond lengths all range around 1.06–1.09 Å. At planar geometries, the two equivalent C–H bonds are longer than the unique one in the ethylenic form and are shorter in the allylic form. Exactly the opposite trend is found for the nonplanar geometries.

In the equilibrium C_s ethylenic form, all the basis sets indicate the unique CH bond to be bent about 45° away from the carbon atom plane. The two equivalent CH bonds are on the same side as the unique one with the smallest and largest basis sets but are on the opposite side in the other two cases. However, the bending is less than 1° in all cases, and it should only be concluded that they are essentially in the plane. In the C_s allylic form all the calculations indicate that the unique CH bond is bent about 5° from the plane and that the two equivalent ones are bent a little over 30°, with all the CH bonds being on the same side of the plane.

The projections of the CH bonds into the carbon plane (see Figure 2) are always close to the respective C–C–C bisectors. The deviation is less than 1° in most cases, the exception being the C_s allylic form where the deviation is about 4°.

The energetic and geometric trends discussed above are similar with all the basis sets considered. It is concluded then that even the minimal STO-3G basis set, when utilized in conjunction with a MCSCF orbital model, is capable of providing a qualitatively correct description of this system.

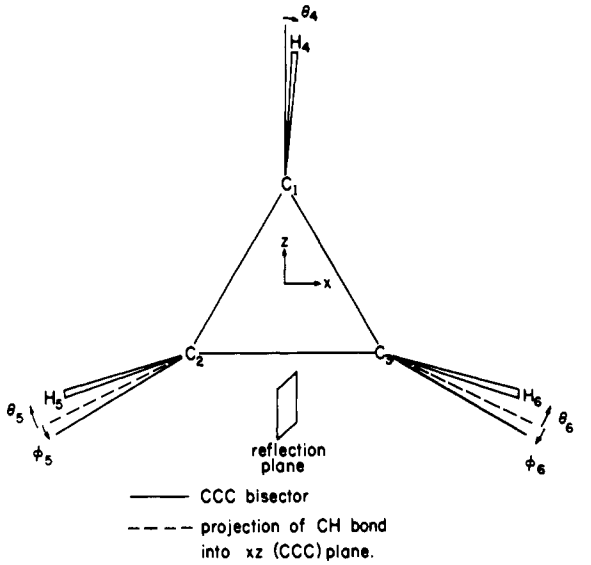

Figure 2. Definition of coordinate axes and geometrical parameters for the description of the cyclopropenyl radical.

IV. Vibrational Analysis of Stationary Points

The geometry optimizations performed above show that the final C_s symmetry ethylenic and allylic forms are stationary points on the potential surface. In this section full vibrational analyses are performed to determine the nature of each stationary point. In particular, it will be shown that the ethylenic form is a local minimum and the allylic form is a transition state.

The vibrational analysis was conducted by displacing each atom in turn by $\pm 0.01\ a_0$ in each Cartesian direction from the stationary point and computing the total energy and analytic gradient at each displaced point. The second derivatives required to construct the Cartesian force constant matrix were obtained by taking finite first differences of the analytic gradients. The Cartesian force constant matrix was then transformed to mass-weighted coordinates and diagonalized to give the normal modes. The six modes corresponding to overall translation and rotation were easily recognized as having frequencies near zero. Dropping these left

Table II. Vibrational Frequencies (cm^{-1}) Calculated at Stationary Points of C_s Symmetry on the Cyclopropenyl Radical Potential Surface with MCSCF/3-21G Wave Functions

mode	ethylenic	allylic
A′ CH bends	616, 1006, 1074, 1235	683, 837, 942, 1132
A″ CH bends	770, 836, 1112, 1186	966, 1044i, 1121, 1267
A′ CC stretches	1659	1520
A′ CH stretches	3315, 3528	3435, 3481
A″ CH stretches	3482	3428

12 normal modes describing the internal vibrational motions. Frequencies obtained for the vibrational normal modes are given in Table II. The last digits reported in the frequencies are probably not significant.

The CH stretching vibrations are all closely clustered in the range of about 3300–3500 cm^{-1}. Taking into consideration the fact that the 3-21G basis set typically gives frequencies about 10–15% above experiment,[17] these can be considered quite normal. The CH bending frequencies cover a somewhat wider range from about 600–1300 cm^{-1}. The only vibrations that are clearly dominated by carbon atom motions are the C=C stretch at 1659 cm^{-1} in the ethylenic form and the C=-C + C-=C stretch at 1520 cm^{-1} in the allylic form.

The descriptions given in Table II for the normal modes are oversimplified, of course, and in each form two of the modes labeled as CH motions also have significant CC components. Among these are a C–C + C–C stretch in the 1235-cm^{-1} ethylenic mode and a C–C stretch in the 1132-cm^{-1} allylic mode. But the most interesting are the carbon atom motions in the 770-cm^{-1} ethylenic mode and in the 1044i-cm^{-1} allylic mode. These correspond to distortions that interconvert the two forms by pseudorotation. The imaginary frequency of the latter indicates that it is not a true vibrational mode—it corresponds to motions that lower the energy by leading back to equilibrium ethylenic forms. The presence of a single imaginary frequency in the allylic form is necessary and sufficient to prove that it is the transition state for pseudorotation, while the occurrence of only positive real frequencies for the ethylenic form proves it to be a local minimum on the potential surface.

The barrier to pseudorotation is then the energy difference between the optimum C_s symmetry ethylenic and allylic forms. Results for the electronic contribution to this barrier have already been discussed above. Another contribution arises from the difference in vibrational zero-point energy $\sum^1/_2 h\nu_i$ in the two forms. Offhand, one would expect this correction to lower the energy barrier, since the transition state has "lost" one vibrational degree of freedom and so should have less zero-point energy. The present calculations indicate that the vibrational contribution does indeed lower the barrier, by 1.5 kcal/mol at the MCSCF/STO-3G level and by 1.4 kcal/mol with MCSCF/3-21G.

V. Pseudorotation Profile

Pseudorotation of the carbon–carbon double bond about the ring is illustrated in Figure 3. Also shown is a convenient "reaction coordinate" ω to describe the motion. Note that ω varies over 360° to repeat identical structures, 120° to relate equivalent structures, and 60° to move from an equilibrium structure to a transition state. In this section, we consider the problem of determining the energy and geometry changes as a function of ω.

The optimized ethylenic and allylic geometries provide values of all the internal coordinates for any value of ω that is an integer multiple of 60°. A unique determination of the geometry for intermediate values of ω is difficult in principle, since several of the internal coordinates undergo large-amplitude changes during pseudorotation. The procedure followed here is eminently reasonable and should provide a qualitatively correct description of the pseudorotation process, although it should be recognized that other approaches are possible.

(17) Pople, J. A.; Schlegel, H. B.; Krishnan, R.; Defrees, D. J.; Binkley, J. S.; Frisch, M. J.; Whiteside, R. A.; Hout, R. F.; Hehre, W. J. *Int. J. Quantum Chem., Quantum Chem. Symp.* **1981**, *15*, 269.

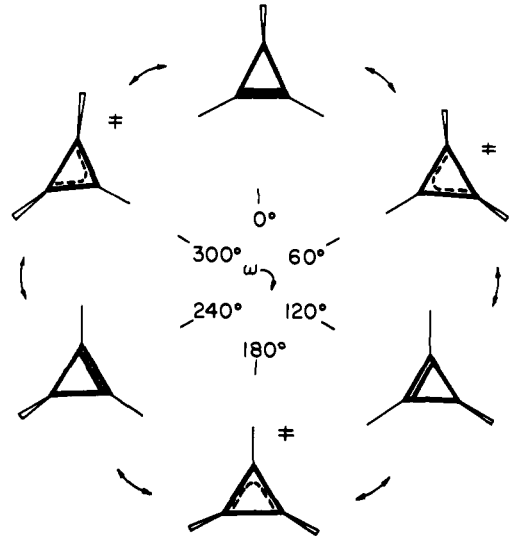

Figure 3. Pseudorotation of the cyclopropenyl radical.

Table III. Fourier Coefficients That Define the C–C Bond Lengths during Pseudorotation of the Cyclopropenyl Radical, As Obtained from Truncation of the Expansions of Eq 1–3 and Fitting to ab Initio MCSCF Calculations with Various Basis Sets

coefficient	STO-3G	3-21G	[32|2]	[321|2]
ρ_0	1.423	1.428	1.439	1.417
ρ_1	−0.092	−0.108	−0.100	−0.094
ρ_2	−0.011	−0.005	−0.006	−0.006
ρ_3	−0.002	−0.000	−0.001	−0.001

The periodicity of the pseudorotation guarantees that each internal coordinate can be expressed as a Fourier series in ω. For example, the three C–C bond lengths can be expanded as

$$R_{23} = \sum_{k=0}^{\infty} \rho_k \cos k\omega \quad (1)$$

$$R_{12} = \sum_{k=0}^{\infty} \rho_k \cos k(\omega - 120°) \quad (2)$$

$$R_{13} = \sum_{k=0}^{\infty} \rho_k \cos k(\omega - 240°) \quad (3)$$

If the infinite series is truncated, the leading four coefficients ρ_k (k = 0, 1, 2, 3) can be found by fitting to the four independent C–C bond lengths obtained from optimization of the ethylenic and allylic geometries. This leads to the results reported in Table III. Examination of the table suggests that the series is converging very rapidly. We take this to indicate that the omitted higher order terms make negligible contributions, so that the truncated series can provide a useful interpolation function for the C–C bond lengths at intermediate values of ω.

Similar treatments of the other independent internal coordinates, which govern the hydrogen atom positions, give Fourier series that do not appear to be rapidly convergent. Thus, at intermediate values of ω the truncated Fourier series procedure was used only to interpolate values of the C–C bond lengths, while the hydrogen atom positions were determined by geometry optimization. This constrained optimization gave the energy profile plotted in Figure 4 and the geometries shown in Figure 5. The MCSCF coefficients of the dominant wave function configuration (after maximizing each to uniquely determine the unitary transformation among the active MCSCF orbitals) were found to vary smoothly with ω from 0.973 for the ethylenic form to 0.941 for the allylic form.

It is seen in Figure 4 that the energy rises only slowly from its initial ethylenic value, and does not become chemically significant until about halfway to the allylic transition state. Also shown there is the vertical excitation energy, obtained as the second CI root calculated with the frozen MCSCF orbitals of the ground state.

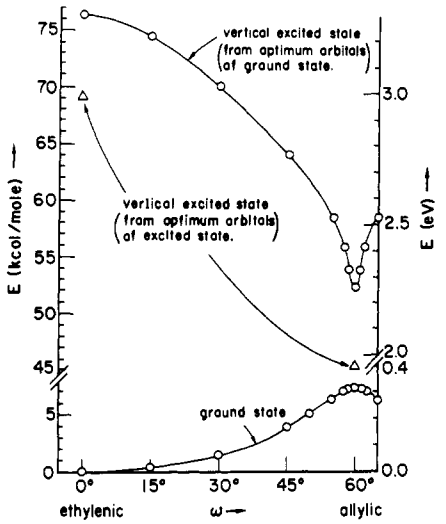

Figure 4. Energy changes during pseudorotation of the cyclopropenyl radical, as obtained from MCSCF/STO-3G calculations.

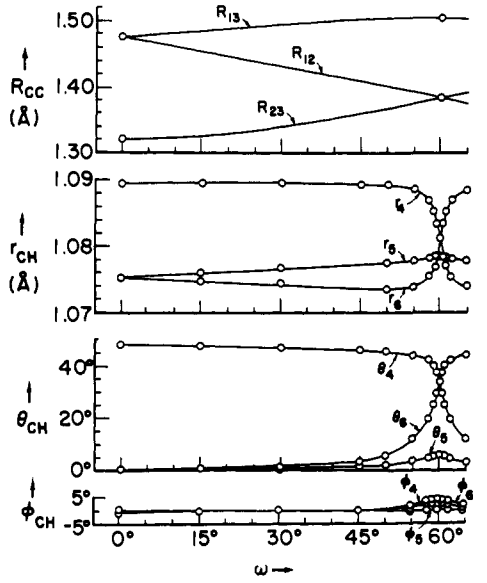

Figure 5. Geometry changes during pseudorotation of the cyclopropenyl radical, as obtained from MCSCF/STO-3G calculations.

At intermediate values of ω all states are of the same symmetry, but at $\omega = 0°$ and 60° C_s symmetry applies and the excited state is of different symmetry than the ground state. This allows for calculations at these two points in which the MCSCF procedure optimizes orbitals for the excited state. Utilizing different (optimized) orbitals for each state was found to lower the ethylenic excited state by 0.32 eV and the allylic excited state by 0.30 eV. Thus, a more balanced description would probably uniformly shift the entire excited state curve down by about 0.3 eV.

In light of the above discussion, the vertical excitation energy is probably about 3 eV at the ethylenic geometry, and about 2 eV or less at the allylic geometry. The absolute energy of the excited state drops nearly 1 eV (over 20 kcal/mol) over this same range. The excited state energy has very high curvature near the allylic point at 60°. In fact, the appearance of the energy curves is reminiscent of an avoided curve crossing, but the large energy gap and lack of symmetry classification at intermediate values of ω precludes any obvious connection.

Figure 5 depicts the geometry changes during pseudorotation. The C–C bond lengths, being dominated by the first two terms in the Fourier expansion, show a gradual change essentially varying as cos ω. Changes in the C–H bond lengths and out-of-plane bending angles are seen to all occur rather suddenly within about 5–10° of the allylic transition state. It is clear that many terms would be required to fit these latter motions to Fourier series in ω. The projections of the CH bonds into the C–C–C plane are seen to vary little from the C–C–C bisectors throughout the entire motion.

VI. Quantitative Determination of the Pseudorotation Barrier

In order to obtain a more truly quantitative determination of the barrier to pseudorotation, large-scale CI calculations were carried out at the optimum MCSCF/[321|2] C_s geometries. Due to program limitations, the size of the [321|2] basis set was reduced by three functions, using only the five true carbon d functions instead of the six nominal d-type functions that were included in the earlier calculations. At the MCSCF level, this raises the ethylenic total energy by 1.13 kcal/mol to −115.2257 au and the allylic total energy by 1.06 kcal/mol to −115.2181 au. The ethylenic–allylic energy difference is then affected by only 0.06 kcal/mol (changing from 4.86 to 4.80 kcal/mol). There should also be a negligible effect at the CI level. The size of the configuration space was also reduced by making a frozen core approximation, not allowing excitations from the three lowest energy MO's that represent the carbon 1s core electrons. Otherwise, all excitations differing by one or two spin orbitals from any of the four configurations occupied in the MCSCF reference space were included. Note that this includes some triple and quadruple excitations relative to the dominant configuration. This SDCI wave-function model incorporated 163 736 and 180 166 space-spin adapted configurations for the ethylenic and allylic geometries, respectively, and led to total energies of −115.5476 au (ethylenic) and −115.5398 au (allylic), a lowering of the total energy of each state by over 200 kcal/mol.

Despite the large CI corrections to the total energies, the energy barrier at the SDCI level was found to be 4.85 kcal/mol, only differing by 0.05 kcal/mol from the MCSCF result in this basis! This surprisingly small CI correction must be fortuitous to some extent. Nonetheless, it provides further convincing evidence that the MCSCF model utilized for most of the calculations is well balanced in the sense that it is capable of describing those electron correlations that are of importance for energy changes along the pseudorotation path of the cyclopropenyl radical.

The energy difference calculated above provides only the electronic contribution to the pseudorotation energy barrier. There is also a contribution from the difference in zero-point vibrational energies of the equilibrium and transition-state structures. As discussed in section IV, this correction lowers the barrier by about 1.4 kcal/mol. Combining this with the electronic contribution discussed above then gives our final best estimate of about 3–4 kcal/mol for the (classical) pseudorotation energy barrier. The quantum mechanical tunneling correction is an open question, but we do not expect it to be large. If this is true, then the 3–4-kcal/mol barrier found here should correlate closely with that measured experimentally. In this connection, it is gratifying that the result agrees well with the experimentally based estimates of 3.5–7 kcal/mol[2] and 3.0–3.5 kcal/mol[18] for the barrier in the trimethyl derivative of the cyclopropenyl radical.

VII. One-Electron Properties

The equilibrium conformation of the cyclopropenyl radical was further characterized by calculating a number of one-electron properties. Of particular interest is the spin density, since this determines the hyperfine coupling constants (hfc) observed in ESR spectroscopy, which is the most promising experimental method for detection of this species. We have previously shown[19] that a full double-ζ basis set including excitations from carbon 1s core orbitals is necessary to describe the important core-electron spin-polarization contributions to ^{13}C hfc. Accordingly, the more flexible [421|2] basis contraction scheme[13] was used and no frozen core approximation was applied in the property calculations. These considerations precluded the calculation of a full SDCI wave

(18) Ingold, K. U., private communication, 1984. This estimate is based on data from ref 3, where it is reported that the rate constant for isomerization changes from ca. 9×10^5 s^{-1} at ca. 104 K to ca. 9×10^8 s^{-1} at ca. 203 K. If one makes the reasonable assumption that log (A/s^{-1}) lies in the range 12.2–13.0, this then implies that $E \approx 3.0$–3.5 kcal/mol.

(19) Chipman, D. M. *J. Chem. Phys.* **1983**, *78*, 3112.

Table IV. One-Electron Properties of Equilibrium Cyclopropenyl Radical, As Obtained from ab Initio MCSCF+SECI/[421|2] Calculations

Dipole Moment μ (D)

μ_x	μ_y	μ_z	$\|\mu\|$
0.00	−0.73	−1.35	1.54

Quadrupole Moment Q at Center of Mass (10^{-26} esu cm^2)

Q_{xx}	Q_{yy}	Q_{zz}	Q_{xy}	Q_{xz}	Q_{yz}
−15.6	−19.4	−18.5	0.0	0.0	−1.3

Electric Field Gradient q at Nucleus (10^{15} esu cm^{-3})

	q_{xx}	q_{yy}	q_{zz}	q_{xy}	q_{xz}	q_{yz}
C_1	0.292	0.214	−0.506	0.000	0.000	0.020
$C_{2,3}$	0.337	−0.913	0.576	0.064[a]	−0.468[a]	−0.113
H_1	0.528	−0.248	−0.280	0.000	0.000	0.793
$H_{2,3}$	−0.669	0.537	0.132	−0.009[a]	−0.724[a]	−0.007

Potential at Nucleus Φ (esu cm^{-1}), Charge Density at Nucleus ρ (au), and Isotropic hfc a (G)

	Φ	ρ	a
C_1	−1.34	119.4	132.1
$C_{2,3}$	−1.33	119.5	−2.0
H_1	−0.100	0.411	32.9
$H_{2,3}$	−0.095	0.405	−5.2

Anisotropic hfc **B** (G)

	B_{xx}	B_{yy}	B_{zz}	B_{xy}	B_{xz}	B_{yz}
C_1	−18.5	29.9	−11.4	0.0	0.0	23.0
$C_{2,3}$	−3.0	5.1	−2.1	−0.7[a]	0.7[a]	4.5
H_1	−9.0	5.0	4.0	0.0	0.0	−6.8
$H_{2,3}$	1.4	−1.0	−0.4	0.0	2.6[a]	0.9

[a] The signs given are appropriate for C_2 or H_2. For C_3 or H_3, the opposite sign applies.

function. However, it was deemed quite sufficient for property calculations to augment the MCSCF reference space with all single excitations (SECI) from any of the four occupied MCSCF configurations.

This led to a SECI wave function with 1822 space-spin adapted configurations, from which one-electron property expectation values were evaluated. Definitions of the property operators have been given previously[19] and so are not repeated here. The coordinate system used is given in Figure 2. Results, obtained at the optimum MCSCF/[321|2] geometry, are reported in Table IV.

Since there are no experimental or previous theoretical results with which to compare, the property calculations must stand as predictions and the discussion will be brief. The dipole moment of 1.5 D is sufficient to expect some dipolar interaction with a solvent or matrix. Experimental measurements of the quadrupole moment, the potentials at the nuclei, the quadrupole coupling constants that are proportional to the electric field gradients at the nuclei, or the charge densities at the nuclei seem unlikely in the foreseeable future.

The isotropic spin densities at the nuclei, reported here as hfc, are probably the most important of the calculated properties. Conversion factors and the method of decomposing into separate direct and spin-polarization contributions have been discussed previously.[19] For the apex hydrogen atom, which is well out of the carbon plane, the 32.9 G result for a(H) is composed of a 33.1 G direct contribution and a very small −0.2 G spin-polarization correction. This is in good agreement with the +37.0 G experimental result[3] found for this hydrogen in the dimethyl derivative. The other two equivalent hydrogen atoms are essentially in the carbon atom plane. Not surprisingly, then, they have very small direct contributions of 0.2 G and larger spin-polarization contributions of −5.3 G to produce the −5.2 G result for a(H). The

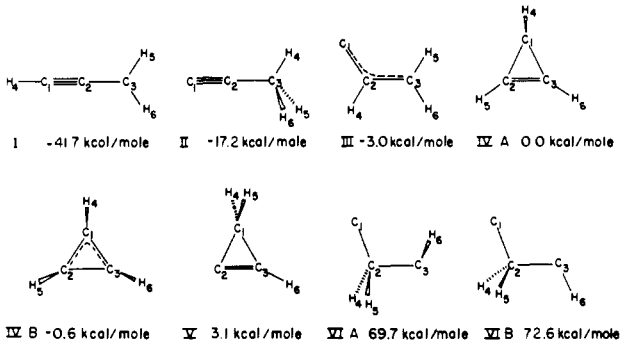

Figure 6. Survey of relative energies of C_3H_3 isomers, as obtained from ab initio UHF/STO-3G calculations.

apex carbon atom has substantial sp hybridization due to bending of the hydrogen atom away from the carbon plane, so one expects a large direct contribution to $a(^{13}C)$ and indeed it is calculated to be 116.8 G. The spin-polarization contribution is calculated to be of the same sign, increasing $a(^{13}C)$ by 15.2 G to a result of 132.1 G. The two equivalent carbon atoms have expectedly small direct contributions of 2.7 G to $a(^{13}C)$ and negative spin-polarization contributions of −4.7 G, giving the −2.0 G net results. In general, spin-polarization contributions are somewhat more difficult to calculate accurately than direct contributions, so the results for the apex carbon and hydrogen atoms are expected to be fairly accurate (probably within 10–20% of experiment, barring any unexpectedly large vibrational averaging corrections) while the errors may be larger for the other atoms.

The anisotropic results are nearly all dominated by direct contributions and so are expected to be fairly accurate. As with the isotropic results, they are largest for the apex hydrogen and carbon atoms and somewhat smaller for the other atoms. They may be of some use in fitting the line shapes of experimental ESR spectra at low temperatures where dipolar broadening must be considered.

Appendix. Survey of C_3H_3 Isomers

In order to gain a more complete qualitative picture of the C_3H_3 potential surface, crude calculations of various isomers were made utilizing the UHF model with the minimal STO-3G basis set. Full geometry optimization was performed for all of the isomers considered. Results are summarized in Figure 6, with energies reported relative to the ethylenic form of cyclopropenyl. Full details of the geometries are reported in Table V.

This survey leaves little doubt that propargyl (I) is the most stable form of the C_3H_3 radical, it being calculated as 42 kcal/mol more stable than ethylenic cyclopropenyl (IVA). Our optimized geometry is in reasonable agreement with that utilized in previous studies[20] of propargyl. Attempts to find a stable allenic-type geometry led back to the propargyl structure. Two other isomers were found to be more stable than cyclopropenyl. Of these, 1-propynl (II) is calculated enough more stable (by 17 kcal/mol) to have confidence in the result. However, the calculated energy lowering of only 3 kcal/mol for structure III is probably too small to allow a definite conclusion to be reached for this form. Inclusion of polarization functions in the basis should stabilize the strained cyclic forms relative to all open-chain forms. Furthermore, the UHF energies of all the isomers except ethylenic cyclopropenyl are artificially lowered by virtue of large spin contamination effects in the wave functions (see $\langle S^2 \rangle$ in Table V, which should be 0.75 for a pure doublet state). Thus, after taking these considerations into account it may well turn out that III is less stable than ethylenic cyclopropenyl (IVA). Optimization of a structure similar to III but with the methylene group twisted by 90° led back to III.

Differential spin contamination effects also lead to an incorrect UHF prediction that the allylic form (IVB) is slightly (0.6 kcal/mol) more stable than the ethylenic form (IVA) of cyclopropenyl itself. More sophisticated calculations reported in the main body of this paper uniformly predict the ethylenic form to be more stable by several kcal/mol. The cyclic structure V is

Table V. Structures of C_3H_3 Isomers, As Obtained from ab Initio UHF/STO-3G Calculations[a]

structure I		structure II		structure III		structure IVA	
R_{12}	1.213	R_{12}	1.219	R_{12}	1.410	$R_{12} = R_{13}$	1.469
R_{23}	1.401	R_{23}	1.489	R_{23}	1.407	R_{23}	1.293
r_4	1.066	$r_4 = r_5 = r_6$	1.089	r_4	1.086	r_4	1.090
$r_5 = r_6$	1.083			r_5	1.081	$r_5 = r_6$	1.076
				r_6	1.081		
$\theta_{235} = \theta_{236}$	121.0	$\theta_{234} = \theta_{235} = \theta_{236}$	110.7	θ_{123}	125.6	$\theta_{214} = \theta_{314}$	127.3
				θ_{124}	115.3	$\theta_{125} = \theta_{136}$	147.7
				θ_{235}	121.4	$\theta_{325} = \theta_{326}$	148.4
				θ_{236}	121.2		
energy	−113.8261	energy	−113.7872	energy	−113.7645	energy	−113.7597
$\langle S^2 \rangle$	1.120	$\langle S^2 \rangle$	1.320	$\langle S^2 \rangle$	1.361	$\langle S^2 \rangle$	0.759
structure IVB		**structure V**		**structure VIA**		**structure VIB**	
$R_{12} = R_{13}$	1.391	R_{12}	1.498	R_{12}	1.549	R_{12}	1.544
R_{23}	1.506	R_{13}	1.519	R_{23}	1.525	R_{23}	1.534
		R_{23}	1.327	θ_{123}	107.8	θ_{123}	109.1
r_4	1.079	$r_4 = r_5$	1.087	r_4	1.090	$r_4 = r_5$	1.093
$r_5 = r_6$	1.081	r_6	1.075	r_5	1.093	r_6	1.104
				r_6	1.104		
$\theta_{214} = \theta_{314}$	146.8	$\theta_{214} = \theta_{215}$	120.0	θ_{124}	111.4	$\theta_{124} = \theta_{125}$	111.4
$\theta_{125} = \theta_{136}$	133.9	$\theta_{314} = \theta_{315}$	119.5	θ_{125}	109.9		
$\theta_{325} = \theta_{326}$	139.0	θ_{136}	143.7	θ_{324}	110.8	$\theta_{324} = \theta_{325}$	108.8
				θ_{325}	108.5		
				θ_{236}	112.4	θ_{236}	111.0
				τ_{1236}	55.1		
energy	−113.7607	energy	−113.7548	energy	−113.6487	energy	−113.6440
$\langle S^2 \rangle$	1.132	$\langle S^2 \rangle$	1.194	$\langle S^2 \rangle$	1.809	$\langle S^2 \rangle$	1.705

[a] See Figure 6 for atom numbering. Distances are given in angstroms, angles in degrees, and energies in atomic units.

calculated to be slightly less stable (3 kcal/mol) than ethylenic cyclopropenyl and would probably become more unstable after correction for spin-contamination effects. The closely related open-chain isomers VIA and VIB are considerably less stable (by ~70 kcal/mol in these calculations) than the cyclopropenyl radical.

In addition to the severe spin-contamination problems for all the other C_3H_3 forms, we find that the UHF method is also unsatisfactory for ethylenic cyclopropenyl itself because of a symmetry instability. At the optimum C_s ethylenic geometry found from C_s symmetry-constrained wave functions, a nonsymmetric wave function was found to give a 0.3 kcal/mol lower energy. Geometry optimization with the nonsymmetric wave function would probably ultimately lead to the allylic form, which does not seem to show any UHF symmetry instability.

In principle, the UHF spin-contamination problem in this system could be rectified by utilizing the ROHF method. Geometry optimizations[9] with ROHF/STO-3G wave functions in C_s symmetry lead to geometries similar to those obtained with UHF/STO-3G, but they give a seriously exaggerated energy result of the allylic form being 20.6 kcal/mol less stable than ethylenic. Also, the ROHF method is well-known to exhibit a symmetry instability for the allyl radical itself[21] and for related allylic-type radicals,[20d] and sure enough one amounting to 1.0 kcal/mol was found here at the optimum C_s allylic geometry of cyclopropenyl. Geometry optimization with the nonsymmetric ROHF wave function would probably ultimately lead back to the ethylenic form, which does not seem to show any ROHF symmetry instability.

From this crude survey, it is possible to draw several important conclusions relevant to cyclopropenyl radical calculations. The existence of several other C_3H_3 isomers close or lower in energy emphasizes the importance of establishing the true nature of any apparent stationary points found on the potential surface. Also, it is clear that Hartree–Fock based methods such as UHF and ROHF exhibit qualitative failures, both with respect to relative total energies and to symmetry instabilities, that eliminate them as reasonable models for study of the potential surface of this system.

Acknowledgment. One of the authors (D.M.C.) gratefully acknowledges the hospitality of Dr. T. H. Dunning and the theoretical group at Argonne National Laboratory during a visit when some of the calculations reported here were performed. Dr. R. Shepard deserves special thanks for providing much assistance in learning to use the Ohio State–Argonne CI programs.

Registry No. I, 2932-78-7; II, 89342-91-6; III, 91948-87-7; IVA, 60512-06-3; V, 19528-44-0; VIA, 91948-88-8.

(20) (a) Bernardi, F.; Camaggi, C. M.; Tiecco, M. *J. Chem. Soc., Perkin Trans. 2* **1974**, 518. (b) Bernardi, F.; Epiotis, N. D.; Cherry, W.; Schlegel, H. B.; Whangbo, M. H.; Wolfe, S. *J. Am. Chem. Soc.* **1976**, *98*, 469. (c) Hinchliffe, A. *J. Mol. Struct.* **1977**, *36*, 162. (d) Hinchliffe, A. *J. Mol. Struct.* **1977**, *37*, 295. (e) Baird, N. C.; Gupta, R. R.; Taylor, K. F. *J. Am. Chem. Soc.* **1979**, *101*, 4531.

(21) Paldus, J.; Veillard, A. *Mol. Phys.* **1978**, *35*, 445.